

# ActiTouch: Robust Touch Detection for On-Skin AR/VR Interfaces

Yang Zhang<sup>1</sup> Wolf Kienzle<sup>2</sup> Yanjun Ma<sup>2</sup> Shiu S. Ng<sup>2</sup> Hrvoje Benko<sup>2</sup> Chris Harrison<sup>1</sup>

<sup>1</sup> Carnegie Mellon University  
5000 Forbes Avenue, Pittsburgh, PA 15213  
{yang.zhang, chris.harrison}@cs.cmu.edu

<sup>2</sup> Facebook Reality Labs  
9845 Willows Rd, Redmond, WA 98052  
{wkienzle, yanjun.ma, shiung, benko}@fb.com

## ABSTRACT

Contemporary AR/VR systems use in-air gestures or handheld controllers for interactivity. This overlooks the skin as a convenient surface for tactile, touch-driven interactions, which are generally more accurate and comfortable than free space interactions. In response, we developed ActiTouch, a new electrical method that enables precise on-skin touch segmentation by using the body as an RF waveguide. We combine this method with computer vision, enabling a system with both high tracking precision and robust touch detection. Our system requires no cumbersome instrumentation of the fingers or hands, requiring only a single wristband (e.g., smartwatch) and sensors integrated into an AR/VR headset. We quantify the accuracy of our approach through a user study and demonstrate how it can enable touchscreen-like interactions on the skin.

## Author Keywords

Touch interaction; Finger tracking; Touch segmentation; Augmented reality (AR); Virtual reality (VR).

## CSS Concepts

Human-centered computing → Human computer interaction (HCI) → Interaction devices.

## INTRODUCTION

Today's augmented and virtual reality systems (AR/VR) generally rely on either handheld controllers (e.g., HTC Vive [14], Oculus Rift and Touch [6]) or in-air bare hand gestures (e.g., Leap Motion [19], Microsoft HoloLens [24]) for user input. Both of these approaches excel at fluid, coarse-grained input, but are weaker at fine-grained interactions, such as typing on a virtual keypad. Indeed, it is rare to see closely packed targets in contemporary AR/VR interfaces, and when they do appear, extra care must be taken by the user.

Permission to make digital or hard copies of all or part of this work for personal or classroom use is granted without fee provided that copies are not made or distributed for profit or commercial advantage and that copies bear this notice and the full citation on the first page. Copyrights for components of this work owned by others than ACM must be honored. Abstracting with credit is permitted. To copy otherwise, or republish, to post on servers or to redistribute to lists, requires prior specific permission and/or a fee. Request permissions from [Permissions@acm.org](mailto:Permissions@acm.org).  
UIST '19, October 20–23, 2019, New Orleans, LA, USA  
© 2019 Association for Computing Machinery.  
ACM ISBN 978-1-4503-6816-2/19/10...\$15.00  
<https://doi.org/10.1145/3332165.3347869>

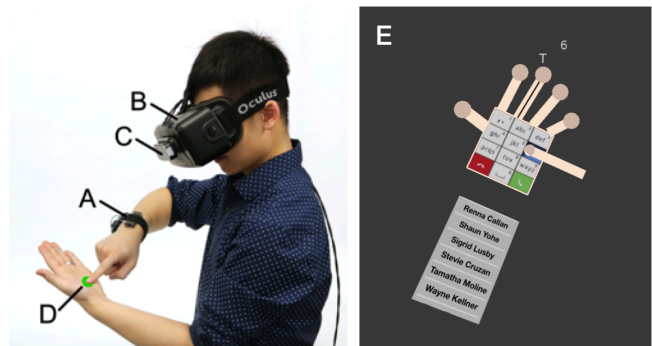


**Figure 1.** ActiTouch enables robust on-skin touch segmentation using a wristband emitter (A) and sensors integrated into an AR/VR headset (B). For spatial tracking of fingers, we use Leap Motion (C) as a proof of concept. Together, this enables precise touch input (D) on the skin for AR/VR interfaces (E).

Fortunately, other input modalities are possible, which can improve the precision, bandwidth and comfort of AR/VR interactions. One such opportunity is input on the skin, which offers a convenient surface for tactile, touch-driven interactions (Figure 1). Prior work has shown that by operating on physical surfaces, users are often more accurate and report higher comfort than equivalent free-space interactions [22]. Further, the ability for users to position arm-borne interfaces as they wish, in concert with increased input precision, affords greater privacy and may be less socially disruptive.

A wide variety of approaches have been considered to enable on-skin input, ranging from wearing a conventional trackpad on the body [32], to worn range-finding sensors [26]. However, most common are systems that use worn cameras and computer vision (e.g., [4, 8, 12, 15, 25, 38]), which are generally very accurate at tracking fingers spatially. OmniTouch [12], which is perhaps the most closely related prior system, offers a useful benchmark: mean Euclidian finger tracking error of 11.9 mm (SD=7.3) on the hand and forearm.

However, a common weakness across camera-based systems is the inability to accurately segment true touches from fingers hovering just above the skin. With visible light (RGB) cameras, there may be no perceivable difference. For this reason, depth cameras are often used, offering distance information that can help disambiguate touching vs. hovering fingers. However, limited depth camera resolution and sensor noise makes this surprisingly challenging [35]. This hover

ambiguity makes end user touch interactions more cumbersome, with users often having to perform exaggerated (z-axis) trajectories to compensate. Again, using OmniTouch as a benchmark, only fingers “above 2 cm were reliably seen as hovering” [12]. Of course, on devices like smartphones, users rarely lift their fingers this high when e.g., typing or scrolling.

In response, we developed ActiTouch, a new electrical method that enables precise, low-latency touch segmentation by using the body as an RF waveguide. Our method complements the spatial tracking strengths of computer vision approaches, enabling a combined system with both high accuracy finger tracking *and* robust touch segmentation. Importantly, our system requires no cumbersome instrumentation of the hands or fingers, requiring only a single wristband (Figure 1A) and a headset (Figure 1B). We quantify the accuracy of our approach through a user study and demonstrate touchscreen-like interactions on the skin in AR/VR.

### RELATED WORK

Our work intersects with two disparate areas of research. Most related to our application domain are systems with on-skin interactivity. Even more closely related to our technical approach are systems that leverage the body’s natural ability to conduct electrical signals for interactive sensing purposes.

### On-Skin Interfaces

The immediacy of skin for on-the-go AR/VR interactivity has drawn attention from the HCI community for over a decade, starting with early work by Karitsuka et al. [15] and Yamamoto et al. [38], both of which used over-the-shoulder cameras and projectors. Many technical approaches have been considered, which we now briefly review.

One option is to directly modify the body, for example, by adding a sensing layer to the skin’s surface, as seen in iSkin [34]. It is also possible to implant sensors under the skin [13], though not all users are comfortable with such instrumentation, and so there has also been much work on less invasive techniques that can sense from afar. For example, the body is a good conductor of sound, and so many projects have utilized bio-acoustics to enable on-body interactions [11, 18, 26]. Acoustic sensing has also been used above the skin for touch input, using e.g., sonar [21].

Optical approaches are also popular, the simplest of which use arrays of infrared proximity sensors integrated into worn devices [16, 36, 37]. Using a fingerprint sensor, SkInteract [28] was able to detect discrete locations on a user’s hand. Many tag-based finger tracking schemes have been used in concert with worn cameras, including retroreflective [15], colored [25] and fiducial markers [29]. PalmBit [38] avoids using markers by tracking the contours of fingers, though only finger-to-finger touches are supported.

Projects such as OmniTouch [12], Imaginary Phone [8] and PalmRC [4] enabled continuous on-skin touch tracking without markers by using depth cameras, though as discussed in the introduction, this approach has other drawbacks. Our

proof-of-concept system also uses computer vision for finger tracking, though we use an off-the-shelf solution (Leap Motion [19]) and combine it with ActiTouch for touch segmentation. As we will show, this combination, though incomplete individually, is potent when unified.

### Body as an Electrical Medium

More closely related to ActiTouch are electrical methods for enabling on-skin interactivity. For example, Potential [23] utilized electromyography (EMG) to detect gestures, while AuraSense [40] used electric field sensing for in-air finger tracking. However, these approaches do not use the body as an electrical medium. ActiTouch takes advantage of the human body’s electrical conductivity, brought to light in the HCI community by papers such as DiamondTouch [5], Humantenna [3], and EMSense [17]. Recently, Varga et al. [33] published an in-depth investigation of this phenomena, focused on implications for Body Channel Communication.

With respect to on-body interactions, there are three projects of particular note. EnhancedTouch [30] and Enhanced TouchX [9] leveraged modulated electrical current to detect human-human touch events, but did not consider a user touching his/her own skin for input. Closest to this work is SkinTrack [39], which used a ring emitter to inject RF into a wearer’s arm when touch contact is made. A smartwatch on the opposing arm contained multiple receiver electrodes that were used to detect and track finger touches by comparing the relative phase of received signals. This arrangement required both hands to be instrumented (i.e., not a single smartwatch, as we propose) and did not consider integration into AR/VR headsets. We also explore a unique fusion between RF sensing and computer vision, leveraging their strengths whilst sidestepping weaknesses.

### SENSING PRINCIPLE

ActiTouch leverages the conductivity of the human body, which conveniently serves as a transmission medium for RF signals. When a user wears an emitter on the arm, the RF signal mainly flows between the two electrodes (P1, Figure 2 left). When a user touches the other arm, a second path (P2) is formed (Figure 2 middle). We also found that P2 increases airborne RF radiation. By placing receiver electrodes in a location that is both along the path of P2 and proximate to airborne radiation, we can use P2 as a touch detection mechanism. Although an ideal setup would be to integrate the receiver into the emitter wristband, we found that proximity to

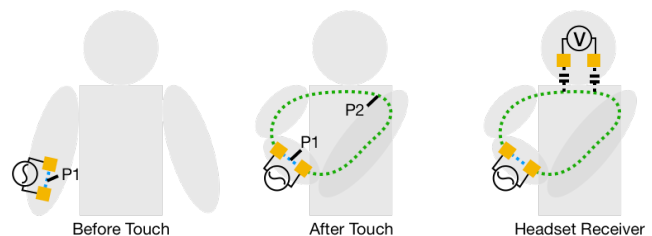


**Figure 2. Dominant RF signal paths before (left) and after touch (middle). The two electrodes on a headset receiver capacitively couple to P2 for touch detection (right).**



Figure 3. Average received signal when the receiver is placed outside (left) and inside (right) the circuit.

P1 provided poor signal-to-noise ratio (SNR). Another possibility is to use a receiver worn on the opposite wrist, but this means users must wear two wrist-worn devices, which is less typical. Instead, we opted to use the head (Figure 2 right), where an AR/VR headset offers an existing platform for instrumentation.

We conducted a basic study to verify our sensing principle (5 participants, 2 female, mean age 24). To better reflect a wearable scenario (i.e., no wall power, small ground plane), we used a battery-powered AD5930 [2] to generate an RF signal and a battery-powered Bluetooth-enabled ADC for measurements. The emitter and receiver used two 2×2 cm copper electrodes attached longitudinally to the user’s arm. The emitter was worn on the wrist of the touching hand, and the receiver sat on the opposite wrist (Figure 3). The emitter was configured to output a 9 Vpp signal at 10.5 MHz (found to be optimal in [10]). Our hypothesis was that placing the receiver inside P2 should yield a stronger received signal.

After wearing the two wristbands, participants were asked to use their right index finger to touch on their opposing palm and forearm. These two locations meant the receiver wristband was *inside* and *outside* P2 respectively (Figure 3). At each touch location, we collected 30 data points with participants touching the skin, and 30 data points with fingers hovering ~1 cm above the skin. We calculated the amplitude difference between touching and hovering as an indicator of P2. We found that when the receiver wristband was outside P2, the on-touch signal delta was 0.21 Vpp on average. When the receiver was placed inside P2, the measured on-touch signal delta increased to 2.30 Vpp. This lends credence to our model, though we caution this is a preliminary result.

### ELECTRODE MATERIAL INVESTIGATION

Efficient and reliable injection of AC signals into the human body requires careful material design of the electrodes. We investigated five materials: copper, copper coated by a thin layer of Kapton tape, silver fabric, dry medical electrode, and wet medical electrode. For each material, we made a pair of 2×2 cm electrodes (except for the dry medical electrode, which came as 1 cm disks). Each pair of electrodes was attached to a user’s skin 10 cm apart. We then inserted a 9 Vpp swept-frequency signal (100 kHz to 12 MHz) with one electrode, while measuring the received signal amplitude from the other electrode. We recruited three participants (1 female,

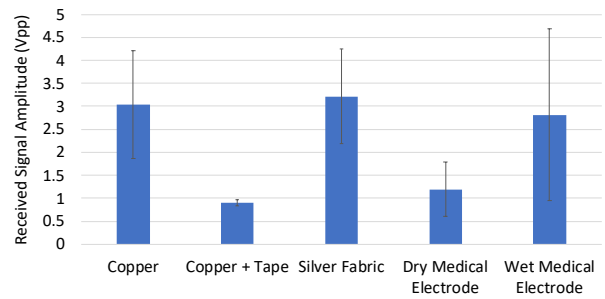


Figure 4. Received signal amplitude across electrode materials. Error bars are standard deviation (variation mostly comes from swept frequency measurements).

mean age 23) and collected data from three body locations: front of the arm, back of the arm, and forehead.

We averaged these results, shown in Figure 4. Among all electrode materials, the silver-based fabric [1] provided the strongest received signal, and thus we adopted it for our final implementation. However, copper with Kapton tape yielded the most consistent response across all signal frequencies and was therefore used for subsequent characterization studies.

### ELECTRODE PLACEMENT INVESTIGATION

The next factor that significantly effects on-body RF sensing is electrode placement, which we also investigated. Prior work has mainly studied two electrode configurations – *capacitive* and *galvanic* – which inspired our electrode placement study design. In a *capacitive* configuration (Figure 5 top), the signal electrode is attached to a user’s skin while the ground electrode is floating, capacitively coupling to earth common ground. In a *galvanic* configuration, both signal and ground electrodes are attached to a user’s body. We studied two arrangements in this configuration – *transversal* and *longitudinal* (Figure 5, middle and bottom). We investigated all pairings of emitter and receiver configurations, resulting in a 3×3 study design (Table 1).

Four participants were recruited for this study (2 female, mean age 24). For all nine emitter-receiver combinations, we configured the emitter to sweep from 100 kHz to 12 MHz at

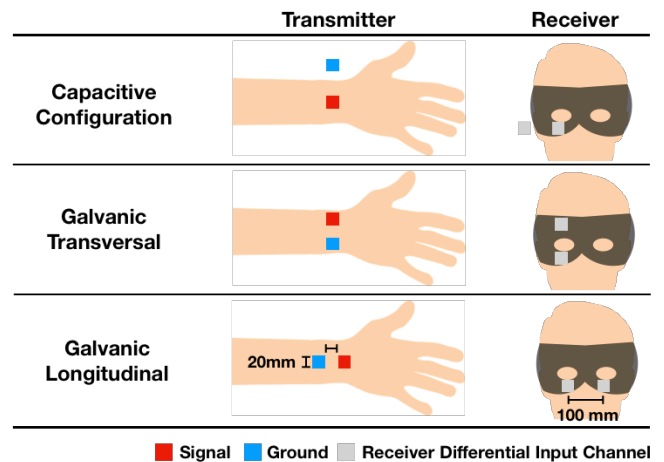


Figure 5. Electrode configurations we studied.

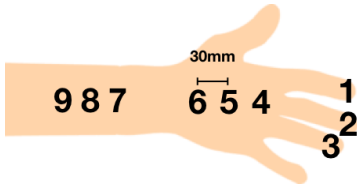


Figure 6. Studied touch locations on the uninstrumented arm.

9 Vpp. We measured the received signal strength at nine touch locations (Figure 6) while the participant was hovering  $\sim 1$  cm above the skin and touching the skin, recording the amplitude before and after touch. Results are shown in Table 1 (combining all participants, touch locations and frequencies for each emitter-receiver configuration). We found the configuration that used the galvanic longitudinal electrode placement for both the emitter and receiver yielded the best on-touch signal. We also used our swept frequency data to confirm 10.5 MHz offered the best SNR.

### SKIN SAFTY INVESTIGATION

To test if ActiTouch is skin-safe, we measured the current inserted into a user’s body using the configuration identified in the previous sections (i.e., galvanic longitudinal,  $2 \times 2$  cm silver fabric electrodes placed 2 cm apart, 10.5 MHz excitation signal frequency). The injected current was estimated by measuring the bio-impedance at the wrist.

Four participants were recruited for this test (1 female, mean age 44). For each participant, we measured the peak and RMS voltages of the open (OC) and closed (L) circuit using a Tektronix MSO58 oscilloscope on the back of the hand and the palm. The bio-impedance is calculated using the measured voltage and the source impedance:

$$Z_{\text{bio}} = Z_s (V_{\text{OC}}/V_L - 1), \text{ where } Z_s = 50 \text{ Ohm.}$$

We measured an average RMS bio-impedance of 420 Ohm ( $SD=266$ ). Thus, the maximum contact current should be  $\sim 10$  mA when the output voltage is configured at 9 Vpp. Despite an extensive search, we did not find any research linking this frequency range and current to negative health effects, though we note that long-term studies are ongoing.

### IMPLEMENTATION

Our proof-of-concept implementation of ActiTouch (Figure 7) required custom electrodes, PCBs, software, and wrist- and head-worn hardware. We now describe each of these components in detail.

#### Electrodes

As previously discussed, we found a silver-based conductive fabric [1] to offer the strongest skin-electrode coupling among the electrode materials we tested. We cut this fabric into small patches that we integrated into two worn components – a wristband emitter and a headset receiver (Figure 7). To electrically connect the fabric to our sensor boards, we used SMA cables soldered to fabric snap fasteners.

#### Emitter Wristband

Our emitter board is built around an AD5930 signal generator chip [2]. To interface with this chip, we used a Freescale

		Transmitter		
Receiver		Galvanic Longitudinal	Galvanic Transversal	Capacitive Configuration
Galvanic Longitudinal		3.69	1.93	2.92
Galvanic Transversal		0.72	0.23	0.95
Capacitive Configuration		0.81	1.04	2.40

Table 1. Average on-touch signal delta for our various electrode configurations (unit mVpp).

K20P64M72SF1 microcontroller [7] running at 96 MHz with Teensy firmware [27]. The AD5930 is configured to output a 10.5 MHz signal at 200 mVpp. We remove the DC component and amplify this signal to 9 Vpp. The board is powered by a 3.7 V lithium ion polymer battery. For electrodes we use two  $2 \times 2$  cm silver-fabric electrodes with a 2 cm spacing. All of these components are affixed to an elastic Velcro strap worn on the wrist (Figure 7, left two images).

#### Receiver Headset

Our receiver board features a two-stage differential signal amplification analog frontend with a gain of 10, built around a LT1806 opamp [20]. The amplified signal is then DC biased to 1.5 V with a voltage reference chip [31] and sampled at 2 MHz by our microcontroller’s built-in ADC. Due to under-sampling, we actually measure an alias of our 10.5 MHz emitted signal. Raw measurements are sent to a laptop over Bluetooth at 50 FPS for additional processing (described next). The receiver board is powered by a 3.7 V lithium ion polymer battery. For electrodes, we found the soft region below the eyes to offer the most reliable skin-to-electrode contact (see Figure 7, headset receiver, side view).

#### Touch Tracking Pipeline

Our touch tracking software runs on a 4-core Intel i7 laptop. After our software receives measurements from our receiver board over Bluetooth, it computes an FFT (non-overlapping window of size 128). We use the FFT bin that contains 10.5 MHz as the RF signal strength indicator for touch segmentation. Due to changes in user posture and varying proximity of the hands to the head, it is not possible to use the raw amplitude of the received signal for touch detection. Instead, we use the first derivative – a sudden and significant increase in signal amplitude indicates a *Finger Touch Down* event, whereas a sudden decrease indicates a *Finger Touch Up* event. This signal is sufficiently clean and characteristic that we can use fixed thresholds with basic hysteresis.

To track a user’s fingers and arms in 3D, we used a Leap Motion [19] camera (Orion SDK) attached to the front of our headset. Specifically, we track the index finger and its distance to the opposing palm and arm planes. If the finger gets

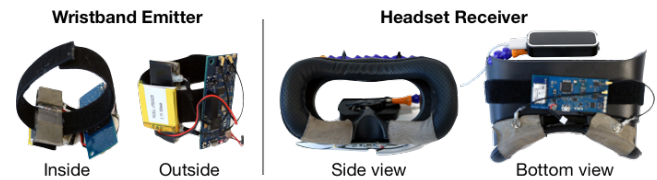
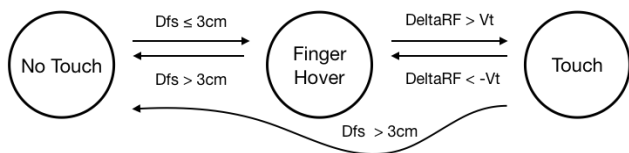


Figure 7. ActiTouch wristband (left two images) and headset (right two images).



**Figure 8. Overview of touch segmentation algorithm. Dfs is the Leap-Motion-reported distance between the fingertip and palm/arm surface; DeltaRF is the first derivative of the received amplitude; Vt is the transition threshold.**

closer than 3 cm to one of these interactive planes, the detection pipeline changes from *No Touch* to a *Finger Hover* state. While in this state, if the first derivative of the received signal is above a threshold, the system moves to a *Finger Touch* state. If the first derivative exceeds a second, negative threshold, the system moves back to a *Finger Hover* state. If the finger moves further than 3 cm away from either the palm or arm, the state returns to *No Touch*. Figure 8 offers an overview of this algorithm.

### Latency

To measure the touch segmentation latency of ActiTouch, we took repeated measurements with a high-speed camera. End-to-end latency – from the moment the finger touches the skin to the instant the computer displays the touch event – was 141 ms on average. In the future, this could be improved by forgoing Bluetooth transmission and laptop processing, and instead performing all compute on processors found in newer AR/VR headsets.

### USER STUDY

To evaluate ActiTouch tracking performance, we ran a user study with 10 participants (2 female, mean age 26, all right handed). This took approximately one hour and participants received \$10 for their time.

We considered several options for ground-truthing touch events, including a Vicon optical tracking setup and a side-mounted depth camera. However, we found in piloting there were significant challenges due to finger curl and angle of attack, as well as complex geometry at the point of contact that necessitated sub-millimeter tracking. Fortunately, we found that human observers were surprisingly accurate, as they could observe the kinematics of finger impacts and the reaction of the limb being touched (e.g., skin deformation, deflection of the limb). For these reasons, we used human observers to confirm touch events in the study.

### Procedure

We evaluated ActiTouch at three body locations: palm, back of the hand, and inside of the forearm. These areas are relatively flat and sufficiently large for touch interactions. After a brief participant orientation, we drew 30mm-interval crosshairs on the three body locations – 3×3 for the palm and back of the hand, and 2×4 for the forearm (Figure 9). We then asked participants to wear our headset and wristband. The headset was hollowed-out (i.e., no screen; Figure 7) so that participants could see their arms. This was done to remove confounding experimental effects, such as VR latency and tracking offsets.

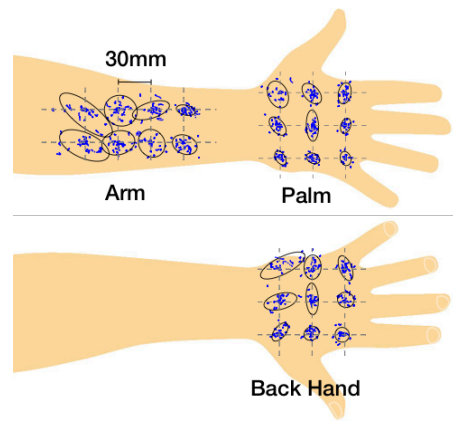


**Figure 9. Requested touch locations (dashed crossings) and the tracked touch points (blue dots) from all participants. Also shown are 2σ confidence ellipses for each crosshair.**

We tested the three body locations sequentially, in a random order. For each location, we collected three rounds of data, and in each round, we collected 10 data points for each crosshair. Crosshairs were automatically requested on an adjacent laptop screen. After the experimenter confirmed the participant performed a touch (note the detected touch state was hidden from both the participant and experimenter), the experimenter advanced the study software to the next trial. The experimenter only intervened if a trial was not performed as requested (e.g., wrong crosshair was touched).

After *Touch* data was collected, we attached a small 5mm-tall transparent acrylic (i.e., not conductive) cylinder to the participant’s fingertip and repeated the above procedure (note this cylinder was fully occluded by the finger and not visible from the perspective of the Leap Motion). This session collected *Hover* data so that we could investigate false positive instances when the finger was very close, but not touching the skin.

In total, this procedure (10 participants × 26 crosshairs × 3 rounds × 10 data points) yielded 7800 *Touch* and 7800 *Hover* trials. Only live touch state output by ActiTouch was recorded (i.e., no post hoc calibration or processing).

### Touch Segmentation Accuracy

On average, ActiTouch achieved a touch segmentation accuracy of 93.8% (SD=2.0). Figure 10 shows the accuracy broken out by body location. Of the errors, 24.2% were false negatives (i.e., *Touch* recognized as *Hover*) and 75.8% were false positives (i.e., *Hover* recognized as *Touch*).

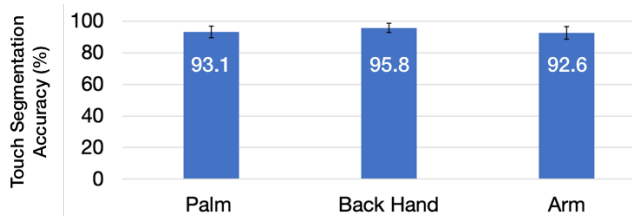


**Figure 10. Touch segmentation accuracies across our three body input locations. Error bars are standard deviation.**

As one point of comparison, we ran a post hoc touch segmentation analysis using only the 3D data reported by the Leap Motion (i.e., a CV-only approach). We varied the touch/hover threshold from 1 to 50 mm (in 1 mm increments) and re-ran our logged data. The best average touch segmentation accuracy achieved (i.e., assuming the ideal threshold was known *a priori*) was 55.5% (SD=1.6).

### Touch Tracking Accuracy

We also evaluated the touch tracking spatial precision of our combined ActiTouch plus Leap Motion pipeline. To calibrate the Leap Motion, we used the first touch trial on each crosshair from each participant to compute a calibration matrix for each body location, which we applied to that participant’s study data. We then calculated the Euclidian distance error between the *reported* touch locations and the *actual* requested touch locations. We included false positives trials (i.e., hover trials detected as touches) to better reflect real world performance. We found that ActiTouch achieved a mean distance error of 5.3 mm (SD=1.1). Figure 9 plots all touch trials from our 10 participants, along with 97.8% (mean + 2σ) confidence ellipses.

### Supplemental Study: Continuous Drawing

To test the continuous touch tracking capability of ActiTouch, we asked the same group of participants to draw five different shapes on their palms (Figure 11, top left), repeated three times each, as naturally as they would on a conventional touchscreen. The crosshairs drawn on the skin from the previous study were used as guides to provide a unified scale. Figure 11 shows the raw drawn paths superimposed from all participants, with no post-hoc corrections or per-user calibration.

### Supplemental Study: Wristband Receiver

Finally, we ran a variant of our study that used a wrist-worn receiver (worn on the opposite arm to the wrist-worn emitter), instead of the receiver integrated into a headset. This study used the same procedure as our main study, as well as the same set of participants. In this arrangement, ActiTouch achieved a mean touch segmentation accuracy of 95.8% (SD=2.3), with a mean tracking distance error of 4.3 mm (SD=0.7). This is slightly more accurate than our headset

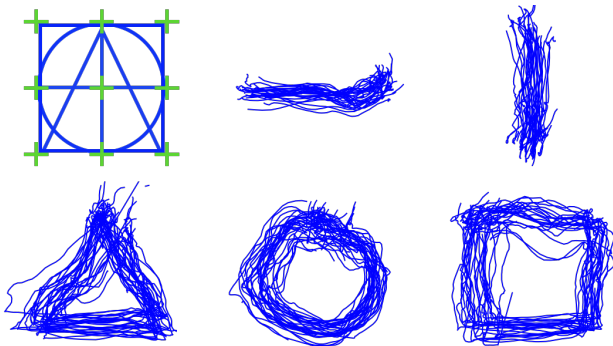


Figure 11. Requested shapes superimposed (top left) onto the crosshairs (green) that were drawn on participants’ palms. Remainder of figure are paths drawn by all participants with no post-hoc or per-user calibration.

receiver, though this arrangement requires instrumentation of both wrists, which as noted earlier, is less desirable.

### EXAMPLE APPLICATIONS

To illustrate the utility of our system, we created three example applications: a dial pad, a music player, and a drawing app. Similar on-skin interfaces have been demonstrated in prior work, but our versions of these applications feature denser interactors, taking advantage of ActiTouch’s high touch segmentation accuracy. Please also see Video Figure.

Our dial pad app, seen in Figure 1, is automatically placed on the palm and features the standard 3×4 grid of buttons. On the longer forearm region, we place a scrollable list of contacts. A scroll bar for fast alphabetical navigation is located on the middle finger. Figure 12 (top) shows a screenshot of our music player application, which uses contemporary scrolling and swiping gestures to navigate between songs, as well as buttons for pause/play and volume control. Finally, we created a drawing app (Figure 12, bottom) to highlight fine grained continuous tracking (beyond directional swipes). In addition to the main canvas area on the palm, the fingers are used as buttons (save, pause/play, erase/paint toggle) and sliders (controls for brush thickness, brush color).

### DISCUSSION

Despite respectable touch segmentation accuracy, ActiTouch has several notable limitations. First, good skin-electrode contact is key to achieving strong and reliable RF signal; if users prefer looser fitting of the wristband or headset, there will be a reduction in performance. Second, although multi-finger touches result in stronger received signal than single-finger touches, our current system cannot reliably distinguish these two events. One potential workaround is to

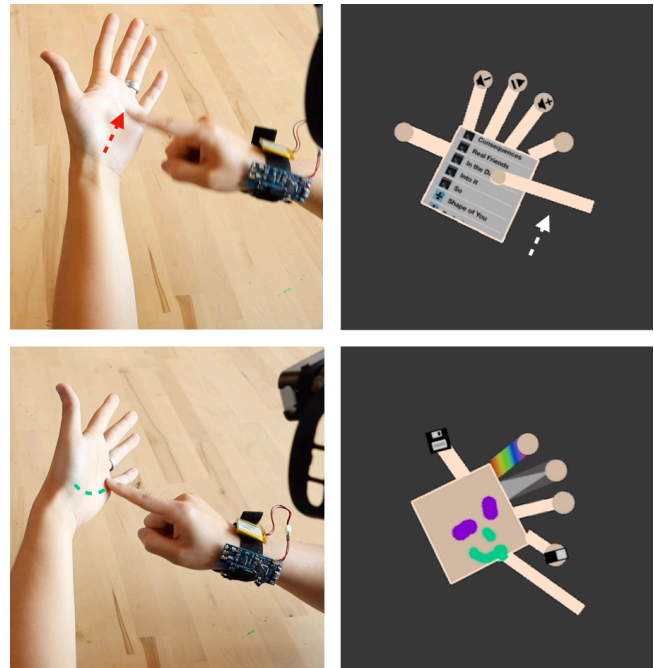


Figure 12. Example applications: a music player (top), and a drawing app (bottom). See Figure 1 for dial pad app.

leverage computer vision, which could predict the number of touching fingers based on hand pose.

As our headset receiver is sensitive to airborne radiation from the emitter, some poses (especially those that bring the arms closer to the head) cause interference. For this reason, we used the first derivative of the received signal, as poses tend to change less rapidly than the instantaneous touching of a finger to the skin. Nonetheless, we still encountered false positives, and this remains an obstacle for future work. Likewise, the amplitude of the first derivative was impacted by user pose and distance between emitter and receiver, and thus a dynamic threshold should be employed in future systems. Finally, we found that touching large conductive surfaces (e.g., laptops, magnetic whiteboards, appliances with metal enclosures) amplified the received signal. In the future, this effect might be used to support on-world touch interactions.

## CONCLUSION

Skin is a convenient and comfortable touch input surface for AR/VR interactions, where contemporary input approaches are generally performed in free space, limiting precision. To advance this vision, we developed ActiTouch, a novel touch segmentation technique that uses the human body as an RF waveguide. Users need only wear one wristband emitter (which could be integrated into future smartwatches) and a head-worn receiver (which can be easily incorporated into AR/VR headsets). We conducted a series of investigations to characterize RF signal propagation in the body, as well as optimize electrode material and placement. We also ran a user study to evaluate the performance of ActiTouch, using a Leap Motion as an exemplar computer vision system to provide finger tracking data. Our results show a mean touch segmentation accuracy of 93.8% and a mean tracking error of 5.3 mm. While future work remains, we believe ActiTouch illuminates a promising new way to enable robust touch sensing in a practical form factor.

## REFERENCES

- [1] Adafruit. Knit Conductive Fabric. Retrieved July 4, 2019 from <https://www.adafruit.com/product/1167>
- [2] Analog Devices. AD5930. Retrieved July 4, 2019 from <https://www.analog.com/media/en/technical-documentation/data-sheets/ad5930.pdf>
- [3] Gabe Cohn, Daniel Morris, Shwetak Patel, and Desney Tan. 2012. Humantenna: using the body as an antenna for real-time whole-body interaction. In *Proceedings of the SIGCHI Conference on Human Factors in Computing Systems (CHI '12)*. ACM, New York, NY, USA, 1901-1910. DOI: <https://doi.org/10.1145/2207676.2208330>
- [4] Niloofar Dezfali, Mohammadreza Khalilbeigi, Jochen Huber, Florian Müller, and Max Mühlhäuser. 2012. PalmRC: imaginary palm-based remote control for eyes-free television interaction. In *Proceedings of the 10th European Conference on Interactive TV and Video (EuroITV '12)*. ACM, New York, NY, USA, 27-34. DOI: <https://doi.org/10.1145/2325616.2325623>
- [5] Paul Dietz and Darren Leigh. 2001. DiamondTouch: a multi-user touch technology. In *Proceedings of the 14th annual ACM symposium on User interface software and technology (UIST '01)*. ACM, New York, NY, USA, 219-226. DOI: <http://dx.doi.org/10.1145/502348.502389>
- [6] Facebook Inc. Oculus Rift and Touch. Retrieved July 4, 2019 from <https://www.oculus.com/rift/accessories>
- [7] Freescale. K20P64M72SF1. Retrieved 7/4/19 from [http://cache.freescale.com/files/32bit/doc/data\\_sheet/K20P64M72SF1.pdf](http://cache.freescale.com/files/32bit/doc/data_sheet/K20P64M72SF1.pdf)
- [8] Sean Gustafson, Christian Holz, and Patrick Baudisch. 2011. Imaginary phone: learning imaginary interfaces by transferring spatial memory from a familiar device. In *Proceedings of the 24th annual ACM symposium on User interface software and technology (UIST '11)*. ACM, New York, NY, USA, 283-292. DOI: <https://doi.org/10.1145/2047196.2047233>
- [9] Taku Hachisu, Baptiste Bourreau, and Kenji Suzuki. 2019. EnhancedTouchX: Smart Bracelets for Augmenting Interpersonal Touch Interactions. In *Proceedings of the 2019 CHI Conference on Human Factors in Computing Systems (CHI '19)*. ACM, New York, NY, USA, Paper 321, 12 pages. DOI: <https://doi.org/10.1145/3290605.3300551>
- [10] Keisuke Hachisuka, Teruhito Takeda, Yusuke Terauchi, Ken Sasaki, Hiroshi Hosaka, and Kiyoshi Ito. Intra-body data transmission for the personal area network. *Microsystem Technologies* 11, no. 8-10 (2005): 1020-1027.
- [11] Chris Harrison, Desney Tan, and Dan Morris. 2010. Skininput: appropriating the body as an input surface. In *Proceedings of the SIGCHI Conference on Human Factors in Computing Systems (CHI '10)*. ACM, New York, NY, USA, 453-462. DOI: <https://doi.org/10.1145/1753326.1753394>
- [12] Chris Harrison, Hrvoje Benko, and Andrew D. Wilson. 2011. OmniTouch: wearable multitouch interaction everywhere. In *Proceedings of the 24th annual ACM symposium on User interface software and technology (UIST '11)*. ACM, New York, NY, USA, 441-450. DOI: <https://doi.org/10.1145/2047196.2047255>
- [13] Christian Holz, Tovi Grossman, George Fitzmaurice, and Anne Agur. 2012. Implanted user interfaces. In *Proceedings of the SIGCHI Conference on Human Factors in Computing Systems (CHI '12)*. ACM, New York, NY, USA, 503-512. DOI: <https://doi.org/10.1145/2207676.2207745>
- [14] HTC. Vive. Retrieved July 4, 2019 from <https://www.vive.com/us/>
- [15] Toshikazu Karitsuka, and Kosuke Sato. "A wearable mixed reality with an on-board projector." In *The*

- Second IEEE and ACM International Symposium on Mixed and Augmented Reality*, 2003. Proceedings., pp. 321-322. IEEE, 2003.
- [16] Gierad Laput, Robert Xiao, Xiang 'Anthony' Chen, Scott E. Hudson, and Chris Harrison. 2014. Skin buttons: cheap, small, low-powered and clickable fixed-icon laser projectors. In *Proceedings of the 27th annual ACM symposium on User interface software and technology (UIST '14)*. ACM, New York, NY, USA, 389-394. DOI: <https://doi.org/10.1145/2642918.2647356>
- [17] Gierad Laput, Chouchang Yang, Robert Xiao, Alanson Sample, and Chris Harrison. 2015. EM-Sense: Touch Recognition of Uninstrumented, Electrical and Electromechanical Objects. In *Proceedings of the 28th Annual ACM Symposium on User Interface Software & Technology (UIST '15)*. ACM, New York, NY, USA, 157-166. DOI: <https://doi.org/10.1145/2807442.2807481>
- [18] Gierad Laput, Robert Xiao, and Chris Harrison. 2016. ViBand: High-Fidelity Bio-Acoustic Sensing Using Commodity Smartwatch Accelerometers. In *Proceedings of the 29th Annual Symposium on User Interface Software and Technology (UIST '16)*. ACM, New York, NY, USA, 321-333. DOI: <https://doi.org/10.1145/2984511.2984582>
- [19] Leap Motion Inc. Leap Motion. Retrieved July 4, 2019 from <https://www.leapmotion.com>
- [20] Linear Technology. LT1806. Retrieved July 4, 2019 from <https://www.analog.com/media/en/technical-documentation/data-sheets/18067fc.pdf>
- [21] Rong-Hao Liang, Shu-Yang Lin, Chao-Huai Su, Kai-Yin Cheng, Bing-Yu Chen, and De-Nian Yang. 2011. SonarWatch: appropriating the forearm as a slider bar. In *SIGGRAPH Asia 2011 Emerging Technologies (SA '11)*, Article 5, 1 pages. DOI: <http://dx.doi.org/10.1145/2073370.2073374>
- [22] Robert W. Lindeman, John L. Sibert, and James K. Hahn. 1999. Towards usable VR: an empirical study of user interfaces for immersive virtual environments. In *Proceedings of the SIGCHI conference on Human Factors in Computing Systems (CHI '99)*. ACM, New York, NY, USA, 64-71. DOI: <http://dx.doi.org/10.1145/302979.302995>
- [23] Denys J. C. Matthies, Simon T. Perrault, Bodo Urban, and Shengdong Zhao. 2015. Potential: Localizing On-Body Gestures by Measuring Electrical Signatures on the Human Skin. In *Proceedings of the 17th International Conference on Human-Computer Interaction with Mobile Devices and Services (MobileHCI '15)*. ACM, New York, NY, USA, 207-216. DOI: <https://doi.org/10.1145/2785830.2785859>
- [24] Microsoft. HoloLens 2. Retrieved July 4, 2019 from <https://www.microsoft.com/en-US/hololens>
- [25] Pranav Mistry, Pattie Maes, and Liyan Chang. WUW-wear Ur world: a wearable gestural interface. In *CHI'09 extended abstracts on Human factors in computing systems*, pp. 4111-4116. ACM, 2009.
- [26] Adiyana Mujibiya, Xiang Cao, Desney S. Tan, Dan Morris, Shwetak N. Patel, and Jun Rekimoto. 2013. The sound of touch: on-body touch and gesture sensing based on transdermal ultrasound propagation. In *Proceedings of the 2013 ACM international conference on Interactive tabletops and surfaces (ITS '13)*. ACM, New York, NY, USA, 189-198. DOI: <https://doi.org/10.1145/2512349.2512821>
- [27] PJRC Inc. Teensy 3.2. Retrieved July 4, 2019 from <https://www.pjrc.com/teensy/teensy31.html>
- [28] Manuel Prätorius, Aaron Scherzinger, and Klaus Hinrichs. SkInteract: An on-body interaction system based on skin-texture recognition. In *IFIP Conference on Human-Computer Interaction*, pp. 425-432. Springer, Cham, 2015.
- [29] Nobuchika Sakata, Teppei Konishi, and Shogo Nishida. Mobile interfaces using body worn projector and camera. In *International Conference on Virtual and Mixed Reality*, pp. 106-113. Springer, Berlin, Heidelberg, 2009.
- [30] Kenji Suzuki, Taku Hachisu, and Kazuki Iida. 2016. EnhancedTouch: A Smart Bracelet for Enhancing Human-Human Physical Touch. In *Proceedings of the 2016 CHI Conference on Human Factors in Computing Systems (CHI '16)*. ACM, New York, NY, USA, 1282-1293. DOI: <https://doi.org/10.1145/2858036.2858439>
- [31] Texas Instruments. REF2030. Retrieved July 4, 2019 from <http://www.ti.com/lit/ds/sbos600d/sbos600d.pdf>
- [32] Bruce Thomas, K. Grimmer, J. Zucco, and S. Milanese. 2002. Where Does the Mouse Go? An Investigation into the Placement of a Body-Attached TouchPad Mouse for Wearable Computers. *Personal Ubiquitous Comput.* 6, 2 (January 2002), 97-112. DOI: <http://dx.doi.org/10.1007/s007790200009>
- [33] Virag Varga, Marc Wyss, Gergely Vakulya, Alanson Sample, and Thomas R. Gross. 2018. Designing Groundless Body Channel Communication Systems: Performance and Implications. In *Proceedings of the 31st Annual ACM Symposium on User Interface Software and Technology (UIST '18)*. ACM, New York, NY, USA, 683-695. DOI: <https://doi.org/10.1145/3242587.3242622>
- [34] Martin Weigel, Tong Lu, Gilles Bailly, Antti Oulasvirta, Carmel Majidi, and Jürgen Steimle. 2015. iSkin: Flexible, Stretchable and Visually Customizable On-Body Touch Sensors for Mobile Computing. In *Proceedings of the 33rd Annual ACM Conference on Human Factors in Computing Systems (CHI '15)*. ACM, New York, NY, USA, 2991-3000. DOI: <https://doi.org/10.1145/2702123.2702391>

- [35] Robert Xiao, Scott Hudson, and Chris Harrison. 2016. DIRECT: Making Touch Tracking on Ordinary Surfaces Practical with Hybrid Depth-Infrared Sensing. In *Proceedings of the 2016 ACM International Conference on Interactive Surfaces and Spaces (ISS '16)*. ACM, New York, NY, USA, 85-94. DOI: <https://doi.org/10.1145/2992154.2992173>
- [36] Robert Xiao, Julia Schwarz, Nick Throm, Andrew D. Wilson, and Hrvoje Benko. "MRTouch: adding touch input to head-mounted mixed reality." *IEEE transactions on visualization and computer graphics* 24, no. 4 (2018): 1653-1660.
- [37] Robert Xiao, Teng Cao, Ning Guo, Jun Zhuo, Yang Zhang, and Chris Harrison. 2018. LumiWatch: On-Arm Projected Graphics and Touch Input. In *Proceedings of the 2018 CHI Conference on Human Factors in Computing Systems (CHI '18)*. ACM, New York, NY, USA, Paper 95, 11 pages. DOI: <https://doi.org/10.1145/3173574.3173669>
- [38] Goshiro Yamamoto and Kosuke Sato. PALMbit: A Body Interface Utilizing Light Projection onto Palms. *Inst. Image Information and Television Engineers* 61, no. 6 (2007): 797-804.
- [39] Yang Zhang, Junhan Zhou, Gierad Laput, and Chris Harrison. 2016. SkinTrack: Using the Body as an Electrical Waveguide for Continuous Finger Tracking on the Skin. In *Proceedings of the 2016 CHI Conference on Human Factors in Computing Systems (CHI '16)*. ACM, New York, NY, USA, 1491-1503. DOI: <https://doi.org/10.1145/2858036.2858082>.
- [40] Junhan Zhou, Yang Zhang, Gierad Laput, and Chris Harrison. 2016. AuraSense: Enabling Expressive Around-Smartwatch Interactions with Electric Field Sensing. In *Proceedings of the 29th Annual Symposium on User Interface Software and Technology (UIST '16)*. ACM, New York, NY, USA, 81-86. DOI: <https://doi.org/10.1145/2984511.2984568>